

# PCCP

Accepted Manuscript



This is an *Accepted Manuscript*, which has been through the Royal Society of Chemistry peer review process and has been accepted for publication.

*Accepted Manuscripts* are published online shortly after acceptance, before technical editing, formatting and proof reading. Using this free service, authors can make their results available to the community, in citable form, before we publish the edited article. We will replace this *Accepted Manuscript* with the edited and formatted *Advance Article* as soon as it is available.

You can find more information about *Accepted Manuscripts* in the [Information for Authors](#).

Please note that technical editing may introduce minor changes to the text and/or graphics, which may alter content. The journal's standard [Terms & Conditions](#) and the [Ethical guidelines](#) still apply. In no event shall the Royal Society of Chemistry be held responsible for any errors or omissions in this *Accepted Manuscript* or any consequences arising from the use of any information it contains.



SCHOLARONE™  
Manuscripts

## Effects of Ga-Te interface layer on the potential barrier height of CdTe/GaAs heterointerface

Shouzhi Xi<sup>a,b</sup>, Wanqi Jie<sup>†a,b</sup>, Gangqiang Zha<sup>\*a,b</sup>, Yanyan Yuan<sup>a</sup>, Tao Wang<sup>a,b</sup>, Wenhua Zhang<sup>c</sup>, Junfa Zhu<sup>c</sup>, Lingyan Xu<sup>a,b</sup>, Yadong Xu<sup>a,b</sup>, Jie Su<sup>a</sup>, Hao Zhang<sup>a,b</sup>, Yaxu Gu<sup>a,b</sup>, Jie Ren<sup>a,b</sup> and Qinghua Zhao<sup>a,b</sup>

The interface layer has great significance on the potential barrier height of CdTe/GaAs heterointerface. In this work, electronic properties of the CdTe/GaAs heterostructure prepared by molecular beam epitaxy is investigated in situ with synchrotron radiation photoemission spectroscopy for CdTe thickness ranging from 3.5 to 74.6 Å. During CdTe deposition, As-Te and Ga-Te interface reaction happen and cause the out diffusion of Ga. A stable GaTe interface dipole layer (more than 30Å) hence forms and reduce the potential barrier height by 0.38eV. The potential barrier height is in proportion to the chemical bonding density and thickness of Ga-Te interface layer. The results establish a more fundamental understanding of the influencing mechanism of interface layer on the potential barrier height of CdTe/GaAs heterointerface.

---

<sup>a</sup> State Key Laboratory of Solidification Processing, Northwestern Polytechnical University, Xi'an 710072, P. R. China

<sup>b</sup> Key Laboratory of Radiation Detection Materials and Devices

<sup>c</sup> National Synchrotron Radiation Laboratory, University of Science and Technology of China, Hefei 230029, P. R. China

<sup>†</sup>Email: (W.J.) jwq@nwpu.edu.cn

<sup>\*</sup>Email: (G.Z.) zha\_gq@nwpu.edu.cn

## 1. Introduction

As one of the most important heterostructures, CdTe/GaAs has attracted much attention in a number of important fields<sup>1,2</sup>, such as infrared detectors<sup>3-5</sup>, solar cells<sup>6</sup>, and nuclear radiation detectors<sup>5,7,8</sup>. In addition to these traditional applications<sup>9</sup>, GaAs and CdTe also offer interesting properties for potential applications in spintronics devices<sup>10,11</sup>, such as nuclear spin polarization<sup>12</sup>, electron spin relaxation<sup>13</sup>, spin coherence<sup>14</sup>, and spin injection<sup>15,16</sup>. These applications in addition rely on several unique relationships between GaAs and CdTe, same crystal structure and similar energy band gap<sup>17</sup>, the proper potential barrier height (PBH) at the heterointerface between the two plays a rather important role in device performance<sup>18-20</sup>. CdTe and CdTe/GaAs can be idea buffer layers for HgCdTe infrared detectors grown on the GaAs and Si substrate to integrate focal-plane arrays into Si-based readout electronics<sup>[21]</sup>. The performance of infrared detectors is mainly determined by the carrier generating from HgCdTe across the interface of CdTe/GaAs. In photovoltaic field, CdTe film also can be grown on the GaAs substrate to be solar cell<sup>[22]</sup> and proper PBH at interface of CdTe/GaAs can void the Ohmic contact problem between p type CdTe and metal electrode<sup>[6]</sup>. In a addition, CdTe film grown on the GaAs substrate can also be used as X-ray detector that the low PBH can make the carrier transport easily across the interface enhance the detector performance such as collection efficiency and energy resolution. In other heterostructure system such as ZnTe/GaAs<sup>23</sup>, ZnTe/GaSb<sup>24</sup>, ZnSe/GaAs<sup>25</sup> and SiC/GaN<sup>26</sup>, the PBH also have great impacts on the carrier transportation and carrier density to affect the device performance. The Interface layer generally exist at the heterostructures because the abrupt interfaces are thermodynamically unstable<sup>27</sup>. For practical application, the properties of interface layer is the key factor to determine the PBH<sup>28,29</sup>. Tuning the PBH through interface layer engineering allows more flexibility in designing devices. However, known from previous work, the detailed properties of interface layer of CdTe/GaAs heterostructure are still remain controversy. Several models have been used to describe the CdTe/GaAs interface layer. Cohen-Solal<sup>30</sup> points out that there are two basic unit cells existing at the interface of CdTe/GaAs: tetrahedral 2Ga-Te-As and twin tetrahedral 2Ga-Te-Te-2Ga. Bourrent<sup>31</sup> considers that there is no intermediate compound and the compound Ga-Te may be a transient structure. CdTe and GaAs are called "covalent" materials because their ionicity, which is defined by the difference in electronegativity of the two constituents, is relatively small<sup>32</sup>. Therefore, the valence-state energy is easier to be influenced by the surface state, chemical reaction and atom diffusion, which makes the interface layer formation more complicated.

The investigation of influence of interface layer on the PBH at semiconductor heterostructure has a long history. Several different heterostructures have been investigated with special emphasis on changing PBH through changing the interface layer, such as adjusting the cation/anion ratio of the interface layer<sup>25, 33</sup> and inducing ultrathin interlayer of a given group material<sup>29, 34</sup>. However, to our knowledge, little study has been performed so far on the CdTe/GaAs heterostructure. Moreover, a complete understanding of the PBH evolution as a function of interface layer formation during CdTe film deposition is still lacking. As far as this fundamental problem is concerned, the method of controlling PBH by interface layer engineering will be limited.

In this paper, CdTe/GaAs heterostructure was prepared by molecular beam epitaxy (MBE) and electronic properties of the heterointerface were investigated using synchrotron radiation photoemission spectroscopy (SRPES) with CdTe coverage from sub-monolayer to multilayers. A stable GaTe interface layer is confirmed to

exist at the interface. We find that the PBH height of interface can be tuned by the electrons provided by Ga-Te bonds and thickness variation of GaTe interface layer. The bonding and dipole controlled interface layer model will be used to explain the corresponding evolution of the PBH of CdTe/GaAs heterointerface.

## 2. Methods

### 2.1 Experimental methods

The SRPES experiments were carried out at the Surface Physics Station of the National Synchrotron Radiation Laboratory (NSRL) of China in Hefei. The endstation equipment has been described in detail previously<sup>35</sup>. The analysis chamber is equipped with a VG ARUPS10 electron energy analyzer for SRPES, a twin-anode X-ray gun, and an Ar<sup>+</sup> sputter gun. The energy resolution ( $E/\Delta E$ ) is better than 1000.

The CdTe (001) film used in this study was grown by MBE system. The exact growth conditions have been discussed in detail elsewhere<sup>36</sup>. Briefly, The vacuum of the MBE deposition chamber and the analysis chamber is better than  $10^{-9}$  and  $10^{-10}$  Torr, respectively. A polished n-type GaAs(100) wafer with Si dopant purchased from Hefei Kejing Materials Technology Co., China was used as the substrate. The sample was etched for 10 min with Ar<sup>+</sup> at ionization voltages of 1.0 and 0.5 kV successively, followed by annealing in situ at 500 °C (thermal couple named temperature) for 40 min to obtain an oxygen and contaminant-free surface, the real temperature may exceed 600 °C and higher than others in similar research<sup>37</sup>. After several cycles of treatment, a clean GaAs (100) surface with  $4\times 1$  reconstruction was obtained<sup>37,38</sup>. Then the CdTe thin film was deposited on the GaAs (100) substrate at 460°C using CdTe flux in the MBE chamber. Pressures ranged from the mid  $10^{-9}$  to low  $10^{-8}$  Torr during the CdTe deposition which are lower than previous research like Angelo<sup>39</sup> to obtain smaller growth rate in order to better observing the interface properties at initial stage. The quartz crystal microbalance located at MBE chamber was used to monitor the CdTe deposition rates. The Te4d, Cd4d, Ga3d and As3d PES spectra were collected using the photon energy of 90 eV. The valence band spectra were taken at photon energy of 28 eV. All Fermi levels were fixed using that of Au, acquired from Au foil attached to the sample holder just below the GaAs sample.

### 2.2 Theoretical methods

An ab-initio pseudo-potential method based on DFT was used to simulate the partial density of states (PDOS) of valence band at the CdTe/GaAs interface, as implemented in the Cambridge serial total energy package (CASTEP)<sup>40</sup>. The geometry optimization was carried out using the Broyden–Fletcher–Goldfrab–Shanno (BFGS) routine. The exchange correlation interaction was treated within the generalized gradient approximations (GGA) of Perdew–Burke–Ernzerhof (PBE). All the atoms in the unit cell are fully relaxed until the force on each atom is less than 0.01 eV/Å. A  $6 \times 6 \times 1$  Monkhorst-Pack k-point grid was used for all calculations and a plane-wave basis set with an energy cutoff of 500 eV. The model of CdTe/GaAs interface is shown in Figure 1. The thickness of CdTe with 3 molecular layers is 5.9Å in order to keep consistent with the experiment result. The lattice ratio of CdTe and GaAs is 7: 8 in order to make the small lattice mismatch with a value of 0.26%. The electronic configuration considered Ga4s, Ga4p, As4s, As4p, Te5s, Te5p, Cd5s, and Cd5p. All the parameters were tested to satisfy the convergence criteria.

### 3. RESULTS AND DISCUSSION

The Cd4d and Ga3p core level photoemission spectra of CdTe on the GaAs surface are shown in Figure 2, in which all curves have been normalized to the main emission feature to emphasize the line shape changes. The Ga3d core level moves from the beginning of CdTe deposition and gradually shifts to higher binding energy until the CdTe thickness is reached to 10.5 Å. The full width at half maximum (FWHM) of Ga3d first increases and then decreases during the deposition, indicating that a chemical reaction occurs and a new component forms, as shown in Figure 3. The spectra are fitted with specialized XPS-peak software using a Shirley background and a Voigt (mixed 10% Gaussian and 90% Lorentzian) line shape. The fitting results match well with the experimental results. As can be seen from Figure 3, the binding energy of the new Ga component appears when the CdTe thickness reaches 3.5 Å is found to be about 0.5 eV higher than that of Ga in GaAs and almost stay as a constant during the CdTe deposition. The formation of this new compound can be ascribed to the Ga-Te reaction. The Ga-Te component rapidly dominates the spectra after the CdTe coverage reaches 6.1 Å. The binding energy of the Cd4d core level is almost a constant throughout the whole range of CdTe coverage. With the thickness of CdTe is 20.8 Å, the spin-orbit splitting of Cd4d is clearly resolved, which differing from the substrate and the reacted interface, where the k-space dispersion of the shallow Cd core levels obscured the spin-orbit splitting<sup>41</sup>, indicating the CdTe film finally forms at a more even atomic environment.

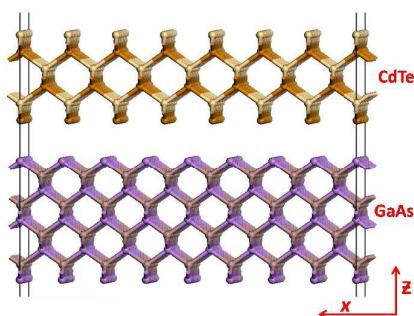


Fig. 1 Optimized geometry of CdTe/GaAs interface with 3 CdTe molecular layers.

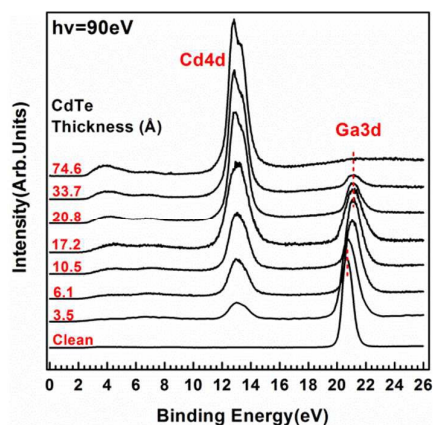
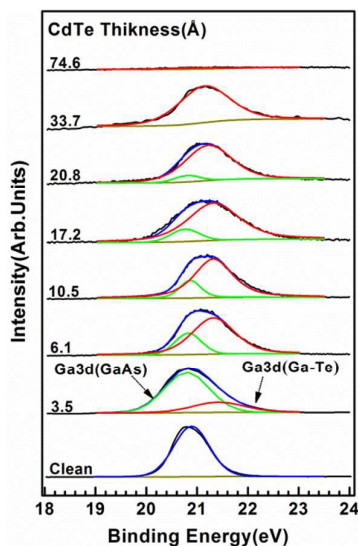
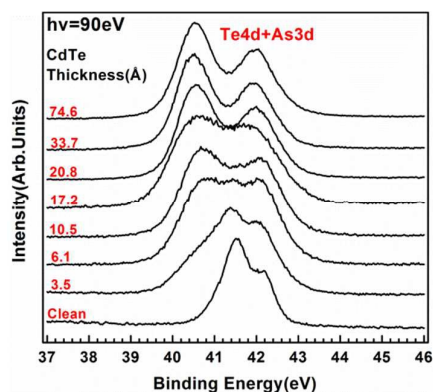


Fig. 2 Cd4d and Ga3d core levels of CdTe/GaAs heterointerface for various CdTe thicknesses measured by SRPES, recorded at normal emission with a photon energy of 90 eV.



**Fig. 3** Evolution of Ga3d core levels of GaAs and Ga-Te reaction at CdTe/GaAs heterointerface for various CdTe thicknesses measured by SRPES, recorded at normal emission with photon energy of 90 eV. Black line: experiment results. Blue line: results of the best fit. Fitted with Ga3d from GaAs (green line) and Ga3d from Ga-Te (red line) components.

The As3d and Te4d core level photoemission spectra of CdTe on the GaAs surface are shown in Figure 4, where all the curves are normalized to the main emission feature to emphasize the line shape changes. The peaks are deconvoluted since the closing peak positions of Te4d and As3d, as shown in Figure 5. The Te4d from CdTe appears at the beginning of CdTe deposition, while new double peaks with 0.2 eV lower binding energy also appears. This new component mainly be ascribed to the As-Te reaction<sup>42</sup> and likely contains weak Ga-Te reaction. The As-Te component almost vanishes with CdTe thickness of 6.1 Å. Simultaneously new double peaks with a 0.23 eV higher binding energy appear and gradually increase. The distance between the two peaks is 0.9 eV less than that for the As-Te component. Te4d from a Ga-Te component is likely responsible for the double peaks. In addition, the binding energy of the two Te4d peaks exhibits different shifts, a discrepancy that may be ascribed to differing relaxation and correlation effects<sup>43</sup>. The Ga-Te reaction may result in the formation of GaTe compound. The heats formation  $H_f$  of CdTe and GaTe are -90.4 KJ/mol and -123.4 KJ/mol, respectively<sup>44</sup>. As a result, GaTe is expected to be more stable at the interface.



**Fig. 4** Te4d and As3d core levels of CdTe/GaAs heterointerface for various CdTe thicknesses measured by SRPES, recorded at normal emission with photon energy of 90 eV.

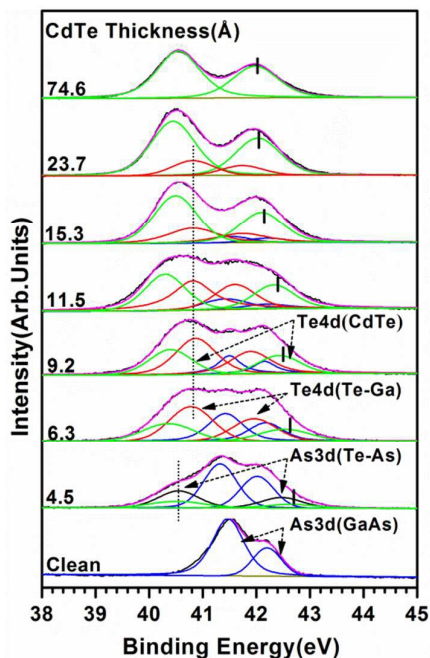


**Fig. 5** Evolution of Te4d and As3d core levels from GaAs, CdTe, As-Te, and Ga-Te reactions at CdTe/GaAs heterointerface for various CdTe thicknesses measured by SRPES, recorded at normal emission with photon energy of 90 eV. Black line: experiment results. Purple line: results of the best fit. Fitted with As3d from GaAs (blue line), As3d from Te-As reaction (black line), Te4d from CdTe (green line), and Te4d from Ga-Te reaction (red line) components.

The sustained Ga-Te reaction should be attributed by the out diffusion of Ga, which can be proved by the evolution of Ga/Te ratio. By calculating the peak area of Ga3d and As4d core levels, the evolution of Ga/Te ratio of the interface is shown in Figure 6. The contents of elements are normalized ranged from [0,1] in order to better comparing the ratio of element at interface region. Consider the error from deconvolution and peak area calculation, results have been recalculated for several times and error bars are added according to the average and standard deviation of fitting process show in Figure 6 and Figure 7. As can be seen from Figure 6, the intensity of As3d is slightly larger than that of Ga3d until the CdTe coverage reaches 10.5 Å. Afterwards, the attenuation of As3d core level is far more rapid than Ga3d. This indicates that Ga out diffusing happens during a certain amount of CdTe deposition, similar results can be seen in ZnSe/GaAs heterointerface<sup>42</sup>. The evolution of the intensity of Te4d and Cd4d core level with CdTe deposition is shown in Figure 7. The intensity of the Te4d signal is larger than that of Cd4d during the whole deposition process. This further proves that Te reacted with the out-diffused Ga to form a stable GaTe interface layer. The Te4d signal from the Ga-Te component still can be observed with the CdTe coverage reached 33.7 Å, as shown in Figure 4. This result indicates that the thickness of GaTe interface layer is more than 30 Å.

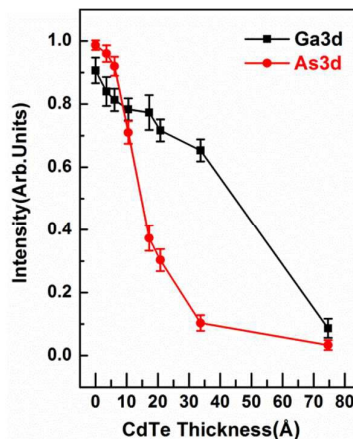


Fig. 6 Evolution of As3d and Ga3d contents at CdTe/GaAs heterointerface for various CdTe thicknesses measured by SRPES.

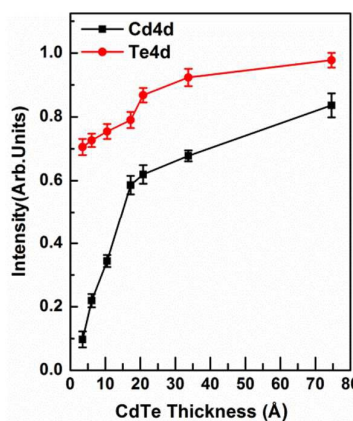


Fig. 7 Evolution of Cd4d and Te4d contents at CdTe/GaAs heterointerface for various CdTe thicknesses measured by SRPES.

The evolution of the valence-band SRPES spectra with CdTe deposition are measured with photon energy of 28 eV, as shown in Figure 8. All of these spectra are normalized to the main emission feature to emphasize the line shape changes. To elucidate the effects of As-Te and Ga-Te chemical reaction on the valence band in detail, the interface densities of states of electrons with 3 CdTe molecular layers are calculated with DFT and shown in Figure 8. The interface model is shown in Figure 1. In order to better comparing with measured results, the horizontal axis has been converted to the reverse direction for the calculation results. The thickness of CdTe layer calculated is 5.9 Å which is similar with the thickness of CdTe at second deposition time for better according with the experimental results. The valence-band maximum (VBM) is chosen as the zero energy reference. As can be seen from Figure 8, the densities of states in the energy ranging from 5.4 to 6.8 eV correspond to the GaAs substrate<sup>45</sup>, and the features observed around 4.4 eV correspond to hybridized Cd 5s and Te 5p orbits originate from CdTe<sup>46</sup>. The densities of As4p and Te5p states overlap obviously in the energy range from 0.2 eV to 0.9 eV, indicating that a hybridization occurs between Te and As, and chemical bonds formation. The valence band ranging from 0.9 eV to 3.5 eV is dominated by As4p, Ga4p and Te5p states. As-Te and Ga-Te reaction should be responsible for these densities of states. The simulation results accord well with the experimental valence band result with the thickness of CdTe is 6.1 Å, which is shown in the upper half of Figure 8. As can be seen, the GaAs

feature gradually attenuates along with the CdTe sustaining deposition. The opposite evolution trend can be seen in the CdTe feature. At CdTe coverage is 3.5 Å, new electronic state related to As-Te reaction can be clearly observed until the CdTe coverage is 10.5 Å which can be ascribed to the Ga out diffusion. The features related to Ga-Te reaction gradually dominate the spectra along with CdTe deposition, which further confirm the sustained Ga-Te reaction occurs at the interface. The valence band maximum (VBM) shown from Figure 8 firstly shifts to the higher binding energy with a value of 0.46eV, then gradually shifts to the lower binding energy with CdTe deposition until a value of 0.38eV is reached. Without other core levels moving, the evolution of the VBM should be ascribed to charge transfer across the interface dipole layer<sup>41, 47</sup> and reflects the evolution of electron PBH which can be calculated by the equation(1),

$$\Delta E_p = \Delta E_c - e\Delta\phi \quad (1)$$

$\Delta E_c$  is the conduct band offset after the CdTe deposition with 3.5Å and the value equals to the difference value of GaAs band gap and VBM.  $\Delta\phi$  is the potential drop at the Ga-Te dipole layer.

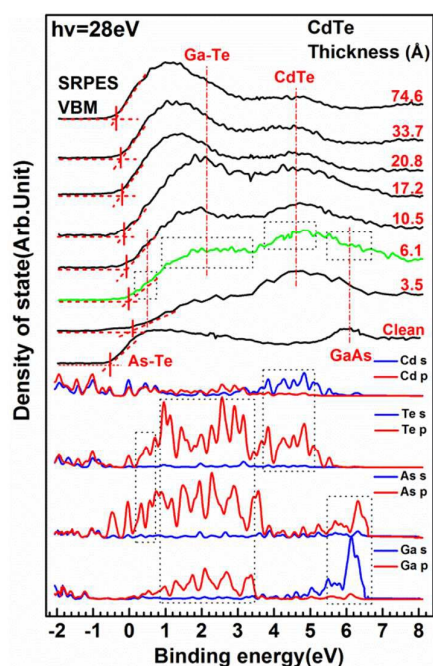


**Fig. 8** Evolution of the valence band of CdTe/GaAs heterointerface for various CdTe thicknesses measured by SRPES compared with calculations of density of states. The SRPES spectra were recorded at normal emission with photon energy of 28 eV. The red and blue solid line is the calculated densities of states. The green solid line is corresponding experimental result. The black solid line is the experiment results with other thicknesses of CdTe.

The evolution of PBH with various CdTe coverage is shown in Figure 9. A large value of 0.46eV is reached and decreases with CdTe sustained deposition, and finally a small value of 0.08eV is reached. The large  $\Delta E_p$  should come from large conduction band discontinuity  $\Delta E_c$  causing by the strong As-Te reaction, which contained Te and As atoms and have relatively large electronegativity. Therefore CdTe deposition will result in a negative dipole

moment at the GaAs surface, which increasing the potential energy of electrons crossing the interface<sup>48</sup> and lead to the large  $\Delta E_c$ . Also, Ga atoms are driven by the negative dipole force to diffuse out and react with Te. Afterwards, the dipole moment changed from negative to positive as Ga out-diffusion and Ga-Te reaction. The electrons provided by Ga-Te reaction will cause a built-in electric field pointing from Ga-Te ( $\delta+$ ) towards GaAs ( $\delta-$ )<sup>49</sup>. Thus, a Ga-Te dipole layer formed at the interface which should be responsible for the reduction of PBH. Accordingly, the energy band alignment of CdTe/GaAs heterointerface is shown in Figure 10. The built-in electric field caused by Ga-Te interface layer makes interface charge situated at a fixed distance inside of the interface. Therefore the Ga-Te interface dipole layer can be considered as a microscopic capacitor<sup>50</sup>. The potential drop at the Ga-Te dipole layer  $\Delta\phi$  is calculated by Equation (2),

$$\Delta\phi = \frac{\sigma d}{\epsilon\epsilon_0} \quad (2)$$

where  $\epsilon$  and  $d$  are the sheet electron density and width of Ga-Te dipole layer. The  $\epsilon$  and  $\epsilon_0$  are the relative dielectric constant of the GaTe and permittivity of vacuum, respectively. The thickness of GaTe layer is 30.2Å,  $\epsilon$  of GaTe is 12.5<sup>51</sup>. Therefore the calculated  $\sigma$  is 1.41E14 cm<sup>-2</sup> per Ga-Te molecular layer with the corresponding maximum  $\Delta\phi$  is 0.38V. The electrons are mainly provided by the Ga-Te bonds formed at dipole layer, each Ga-Te bond have an excess of one quarter electron for the lattice and act as donor<sup>52</sup>. The density of Ga and Te atoms per molecular layer is 4.87E14 cm<sup>-2</sup><sup>53, 54</sup> and the corresponding sheet electron density is 1.22E14 cm<sup>-2</sup>. Therefore Ga-Te bonds mainly dope the interface and make GaTe interface layer a electron accumulation area which will increase the rate of electron tunneling through the GaTe interface layer and hence decrease the PBH<sup>25, 55</sup>. In addition, as the width of Ga-Te interface layer increase, the dipole moment fix more electrons provided by Ga-Te reaction in to the interface area, which increase the potential drop at interface and also decrease the PBH. Therefore, the PBH of CdTe/GaAs heterointerface can be tuned by the electrons provided by Ga-Te bond and the width of Ga-Te interface dipole layer.

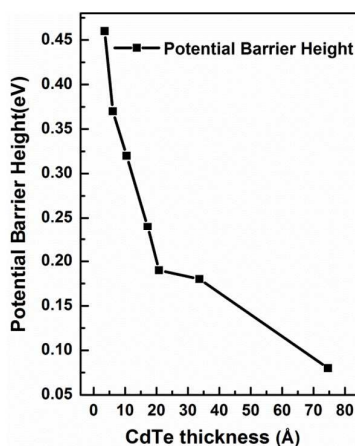


Fig.9 PBH evolution for various CdTe layer thicknesses measured by SRPES.

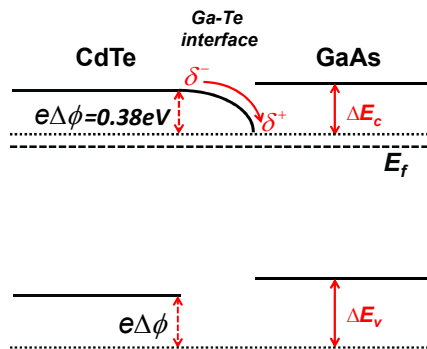


Fig. 10 The schematic of energy band alignment of a CdTe/GaAs heterointerface with Ga-Te interface dipole layer.

#### 4. CONCLUSIONS

Synchrotron radiation photoemission spectroscopy has been used to study the electronic properties of CdTe/GaAs interfaces with CdTe coverage ranging from 3.5 to 74.6 Å. As-Te and Ga-Te strong reaction is found during CdTe deposition. As-Te reaction leads to a negative dipole moment, driving more Ga atoms to out-diffuse and react with Te. The chemical reaction between Ga and Te results in a change in dipole moment from negative to positive and finally forms a stable interface dipole layer, pointing from Ga-Te ( $\delta^+$ ) toward GaAs ( $\delta^-$ ). The Ga-Te bonds formation results in the excess electrons with density of  $1.22 \times 10^{14} \text{ cm}^{-2}$  which has been fixed by the dipole moment and cause a voltage drop inside the Ga-Te dipole layer. The PBH hence reduced with the variation of thickness of Ga-Te layer and a value of 0.38 eV is reached with a 30 Å Ga-Te layer formation. A bonding and dipole controlled interface layer model has been used to explain the PBH reduction. The results provide a guiding direction to control the PBH of “covalent” materials like CdTe/GaAs heterointerface by interface layer engineering and it is very meaningful for the designing of devices.

#### Acknowledgments

This work was supported by the Special Fund of National Key Scientific Instrument and Equipment Development (2011YQ040082), the National Natural Science Foundation of China (50902114, 51372205, 51502244) and the Central Universities Fundamental Research Foundation. The project was also supported by funds from the State Key Laboratory of Solidification Processing in NWPU (SKLSP201219). The authors are grateful to all of the members of NSRL for their help with the experiments.

#### Notes and references

1. A. J. McGibbon, S. J. Pennycook and J. E. Angelo, *Science*, 1995, **269**, 519-521.
2. M. F. Vargas-Charry and C. Vargas-Hernández, *Materials Science in Semiconductor Processing*, 2015, **31**, 561-567.
3. M. Carmody, A. Yulius, D. Edwall, D. Lee, E. Piquette, R. Jacobs, D. Benson, A. Stoltz, J. Markunas, A. Almeida and J. Arias, *Journal of Electronic Materials*, 2012, **41**, 2719-2724.
4. K.-C. Kim, S. Hyub Baek, W. Chel Choi, H. Jae Kim, J. Dong Song and J.-S. Kim, *Materials Letters*,

- 2012, **87**, 139-141.
5. P. J. Sellin, *Nucl. Instrum. Methods Phys. Res., Sect. A*, 2003, **513**, 332-339.
  6. P.-Y. Su, C. Lee, G.-C. Wang, T.-M. Lu and I. B. Bhat, *Journal of Electronic Materials*, 2014, **43**, 2895-2900.
  7. M. Niraula, K. Yasuda, K. Uchida, Y. Nakanishi, T. Mabuchi, Y. Agata and K. Suzuki, *IEEE Electron Device Lett.*, 2005, **26**, 8-10.
  8. A. Raulo, G. Hennard, M. Sowinska, R. B. James, A. Fauler, J. Freier, A. Held and M. Fiederle, *IEEE Trans. Nucl. Sci.*, 2013, **60**, 3815-3823.
  9. N. Lovergine, A. Cola, P. Prete, L. Tapfer, M. Bayhan and A. M. Mancini, *Nucl. Instrum. Methods Phys. Res., Sect. A*, 2001, **458**, 1-6.
  10. O. M. Auslaender, H. Steinberg, A. Yacoby, Y. Tserkovnyak, B. I. Halperin, K. W. Baldwin, L. N. Pfeiffer and K. W. West, *Science*, 2005, **308**, 88-92.
  11. A. Tsukazaki, A. Ohtomo, T. Kita, Y. Ohno, H. Ohno and M. Kawasaki, *Science*, 2007, **315**, 1388-1391.
  12. L. V. Lutsev, *J. Phys. Condens. Matter* 2006, **18**, 5881-5894.
  13. Q. Zhang, Y. Li, D. Pagliero, W. Charles, A. Shen, C. A. Meriles and M. C. Tamargo, *Journal of Vacuum Science & Technology B: Microelectronics and Nanometer Structures*, 2010, **28**, C3D1.
  14. D. Sprinzl, P. Horodyska, N. Tesarova, E. Rozkotova, E. Belas, R. Grill, P. Maly and P. Nemeč, *Phys. Rev. B*, 2010, **82**.
  15. Y. Ohno, D. K. Young, B. Beschoten, F. Matsukura, H. Ohno and D. D. Awschalom, *Nature*, 1999, **402**, 790-792.
  16. H. C. Koo, J. H. Kwon, J. Eom, J. Chang, S. H. Han and M. Johnson, *Science*, 2009, **325**, 1515-1518.
  17. D. Sprinzl, P. Horodyská, N. Tesařová, E. Rozkotová, E. Belas, R. Grill, P. Malý and P. Němec, *Phys. Rev. B*, 2010, **82**.
  18. K. F. Wu, N. H. Song, Z. Liu, H. M. Zhu, W. Rodriguez-Cordoba and T. Q. Lian, *J. Phys. Chem. A* 2013, **117**, 7561-7570.
  19. J. B. Khurgin and I. Vurgaftman, *Appl. Phys. Lett.*, 2014, **104**.
  20. L. J. Brillson, *Surface Science*, 1994, **299**, 909-927.
  21. R. N. Jacobs, J. Markunas, J. Pellegrino, L. A. Almeida, M. Groenert, M. Jaime-Vasquez, N. Mahadik, C. Andrews and S. B. Qadri, *Journal of Crystal Growth*, 2008, **310**, 2960-2965.
  22. R. N. Bicknell, R. W. Yanka, N. C. Giles, J. F. Schetzina, T. J. Magee, C. Leung and H. Kawayoshi, *Applied Physics Letters*, 1984, **44**, 313-315.
  23. P. D. Han, *Defect and Diffusion Forum*, 1999, **174**, 59-65.
  24. C. T. Chou, J. L. Hutchison, D. Cherns, M. J. Casanove, J. W. Steeds, R. Vincent, B. Lunn and D. A. Ashenford, *J. Appl. Phys.*, 1993, **74**, 6566.
  25. A. Frey, U. Bass, S. Mahapatra, C. Schumacher, J. Geurts and K. Brunner, *Physical Review B*, 2010, **82**.
  26. M. Stadele, J. A. Majewski and P. Vogl, *Acta Phys. Pol. A*, 1995, **88**, 917-920.
  27. A. Kley and J. Neugebauer, *Physical Review B*, 1994, **50**, 8616-8628.
  28. G. Biasiol, L. Sorba, G. Bratina, R. Nicolini, A. Franciosi, M. Peressi, S. Baroni, R. Resta and A. Baldereschi, *Physical Review Letters*, 1992, **69**, 1283-1286.
  29. M. Di Ventra, C. Berthod and N. Binggeli, *Physical Review B*, 2005, **71**.
  30. G. Cohen-Solal, F. Bailly and M. Barbé, *Applied Physics Letters*, 1986, **49**, 1519.
  31. A. Bourret, P. Fuoss, G. Feuillet and S. Tatarsenko, *Physical Review Letters*, 1993, **70**, 311-314.

32. S. Kurtin, T. McGill and C. Mead, *Phys. Rev. Lett.*, 1969, **22**, 1433-1436.
33. A. Colli, E. Carlino, E. Pelucchi, V. Grillo and A. Franciosi, *J. Appl. Phys.*, 2004, **96**, 2592.
34. A. Franciosi and C. G. Van de Walle, *Surface Science Reports*, 1996, **25**, 1-+.
35. S. Xi, W. Jie, G. Zha, W. Zhang, J. Zhu, X. Bai, T. Feng, N. Wang, F. Yang and R. Yang, *The Journal of Physical Chemistry C*, 2014, **118**, 5294-5298.
36. G. Bratina, L. Sorba, A. Antonini, G. Ceccone, R. Nicolini, G. Biasiol, A. Franciosi, J. E. Angelo and W. W. Gerberich, *Physical Review B*, 1993, **48**, 8899-8910.
37. J. Massies, P. Etienne, F. Dezaly and N. T. Linh, *Surface Science*, 1980, **99**, 121-131.
38. L. zijiang, Z. xun, W. jihong, G. xiang and D. zhao, *Materials Review*, 2014, **28**, 15-19.
39. J. E. Angelo, W. W. Gerberich, C. Bratina, L. Sorba and A. Franciosi, *Journal of Crystal Growth*, 1993, **130**, 459-465.
40. M. D. Segall, P. J. D. Lindan, M. J. Probert, C. J. Pickard, P. J. Hasnip, S. J. Clark and M. C. Payne, *J. Phys.-Condes. Matter*, 2002, **14**, 2717-2744.
41. X. Bai, W. Jie, G. Zha, W. Zhang, J. Zhu, T. Wang, Y. Yuan, Y. Du, Y. Wang and L. Fu, *J. Phys. Chem. C* 2010, **114**, 16426-16429.
42. G. Bratina, T. Ozzello and A. Franciosi, *Journal of Vacuum Science & Technology a-Vacuum Surfaces and Films*, 1996, **14**, 3135-3143.
43. S. T. Pantelides, D. J. Mickish and A. B. Kunz, *Phys. Rev. B*, 1974, **10**, 5203-5212.
44. I. Barin and G. Platzki, *Thermochemical data of pure substances*, 3rd edn., VCH, Weinheim ; New York, 1995.
45. B. K. Agrawal, S. Agrawal and W. Srivastava, *Surface Science*, 1999, **424**, 232-243.
46. X. Bai, W. Jie, G. Zha, W. Zhang, J. Zhu, T. Wang, D. Qian, Y. Liu and J. Jia, *Appl. Phys. Lett.*, 2013, **102**, 211602.
47. L. Sorba, G. Bratina, G. Ceccone, A. Antonini, J. F. Walker, M. Micovic and A. Franciosi, *Physical Review B*, 1991, **43**, 2450-2453.
48. X. Bai, W. Jie, G. Zha, W. Zhang, J. Zhu, T. Wang, Y. Yuan, Y. Wang, H. Hua and L. Fu, *Chem. Phys. Lett.*, 2010, **489**, 103-106.
49. H.-X. Deng, J.-W. Luo and S.-H. Wei, *Physical Review B*, 2015, **91**.
50. F. Capasso, A. Y. Cho, K. Mohammed and P. W. Foy, *Applied Physics Letters*, 1985, **46**, 664.
51. J. Pellicer-Porres, F. J. Manjon, A. Segura, V. Munoz, C. Power and J. Gonzalez, *Physical Review B*, 1999, **60**, 8871-8877.
52. H. H. Farrell, M. C. Tamargo, J. L. de Miguel, F. S. Turco, D. M. Hwang and R. E. Nahory, *J. Appl. Phys.*, 1991, **69**, 7021.
53. F. Alapini, J. Flahaut, M. Guittard, S. Jaulmes and M. Julienpouzol, *J. Solid State Chem.*, 1979, **28**, 309-319.
54. M. Julien-Pouzol, S. Jaulmes, M. Guittard and F. Alapini, *Acta Crystallographica Section B*, 1979, **35**, 2848-2851.
55. F. Capasso, A. Y. Cho, K. Mohammed and P. W. Foy, *Appl. Phys. Lett.*, 1985, **46**, 664-666.